International Journal of ChemTech Research
CODEN (USA): IJCRGG ISSN: 0974-4290
Vol.7, No.7, pp 2855-2859, 2015

ICEWEST-2015 [05th - 06th Feb 2015]
International Conference on Energy, Water and Environmental Science & Technology
PG and Research Department of Chemistry, Presidency College (Autonomous), Chennai-600 005, India

Humidity sensing studies on $NiWO_4$ – WO_3 composites

M. V. Arularasu[1], S. Poovaragan[1], J. Daisy Rani [2] and R. Sundaram[1]*

[1]PG and Research Department of Chemistry, Presidency College, Chennai - 600 005, India
[2]Department of Chemistry, Jeppiaar Engineering College, Chennai 600 119, India.

Abstract: Experimental results on the composites made from $NiWO_4$ and WO_3 for electrical and humidity sensing properties are described. The composites of nickel tungstate – tungsten trioxide ($NiWO_4$–WO_3) in mole ratios 80:20, 60:40, 40:60 and 20:80 were prepared by high temperature solid state method. The prepared composites characterized by powder X-ray diffraction, EDAX, scanning electron microscope, electrical conductance and humidity sensor studies. Powder XRD pattern of composites showed the presence of $NiWO_4$ and WO_3 phases and EDAX proved the purity of composites. The SEM studies were carried out to study the surface and pores structure of the sensor materials. The composites were subjected to DC conductance measurements as a function of relative humidity in the range of 5 – 98%. The sensitivity factor, S_f ($R_{5\%}/R_{98\%}$) for $NiWO_4$ – WO_3 composites were calculated to be NWWO-82, NWWO-64, NWWO-46 and NWWO-28 is 459, 827, 15535 and 785 respectively. The sensitivity factor of the NWWO-46 composite showed a maximum sensitivity of 15535. NWWO-46 composite exhibits excellent humidity sensing characteristics such as fast response time, rapid recovery.
Keywords: Nickel (II)tungstate, Tungsten trioxide, solid state electrical conductivity and humidity sensor.

Introduction

Transition metal tungstate type compounds have much scientific interest in recent times because of their intriguing properties like electrical and electrochemical property, photoluminescence, photocatalyst, energy storage capacity, and humidity sensing ability[1-5]. Among these tungstates, nickel tungstates have been extensively studied. Mixed nickel tungsten oxide, denote as $NiWO_4$ has important electro chromic properties, besides a high long – lasting structural stability[6] and great catalytic properties[7]. Devices based on nickel oxide and tungsten oxide have been found to exhibit excellent performance[8] and binary nickel – tungstate oxides have been seen to yield properties that are supper to these of the pure oxides both at the tungsten rich[9-10] and at the nickel rich[11-16] ends of the compositional range. Over the last decade, considerable interest has been received to synthesize novel materials with potential humidity sensing characteristics for the fabrication of low cost, rapid and stable humidity sensors[17-20]. An excellent humidity sensor should have high response value, quick response

and fast recovery, good reproducibility, broad range of operational and low cost[21]. Ceramic and polymeric materials have commonly been used as sensing materials for the construction of humidity sensors [22-26].

Experimental

The $NiWO_4$ – WO_3 composites were synthesized from different mol percent $NiWO_4$ and WO_3. A 2 % solution of cetyl alcohol in ethanol was added as an organic binder. The mixture was ground for 6 h in absolute ethanol, dried and compacted into pellets at a pressure of 100 Mpa. The pellets were then heated at a rate of 10 K min^{-1} to 873 K and kept at this temperature for 1 h to remove the binder. Subsequently the temperature was raised to 1023 K at a rate of 2 K min^{-1} where it was maintained for 2 h to facilitate sintering followed by furnace cooling of the samples.

DC measurements and temperature dependence of conductance of the samples were carried out using a two-probe method[27]. Controlled humidity environments for humidity sensing applications were achieved[28] using anhydrous P_2O_5 and saturated aqueous solutions of $CaCl_2.6H_2O$, $Zn(NO_3)_2.6H_2O$, $Ca(NO_3)_2.4H_2O$, $NaNO_2$, NH_4Cl, $BaCl_2.2H_2O$ and $CuSO_4.5H_2O$ in a closed glass vessel at an ambient temperature of 298 K, which yielded 5, 20, 31, 42, 51, 66, 79, 88 and 98 % relative humidity (RH) respectively. The response and recovery characteristics of the humidity sensor was established using a degassed glass chamber having a provision for a two-way inlet, one for transpiring the dry air and the other transpiring moist air stream.

The recovery and response characteristics for humidity sensing was evaluated by using a degassed glass chamber (200 cm^3), which had a provision for two way inlet stopcock, one for transpiring dry air and the other for moist air from a wet candle. The air was dried by transpiring the air stream through drying columns packed with anhydrous $CaCl_2$ and P_2O_5 connected in series. The resistance measurements in dry air as well as in moist air alternatively, helped to establish the recovery and response characteristics for moisture sensing.

Results and Discussion

Figures 1a and 1b show the energy dispersive X-ray spectroscopy (EDAX) analysis and X-ray diffraction (XRD) pattern of the $NiWO_4$ and WO_3 composites respectively. The EDAX analysis shows the expected elements of O, Na, S, Ni, W. The peaks of the EDAX pattern confirm that the product is highly pure. XRD patterns of the tungstates correspond to $NiWO_4$ and WO_3 inferring that there are no impurity phases. In electrical conductivity measurements, the current was found to increase linearly with the applied voltage, indicating the ohmic contacts of the electrodes. The temperature dependence of electrical conductivity was carried out in the temperature range of 323–600 K. The current (I values are given in μA) increased exponentially with respect to temperature from which lnI vs 1/T plot was drawn to determine the activation energy. The activation energy for electrical conduction generally involves the combination of the energy required to raise the carriers from their dominant levels to their corresponding transport bands and the energy required to create the carriers in the dominant levels[29] if they are not already supplied by other means. From the temperature dependence conductivity data, a ln$I$ vs 1/T plot the activation energy was calculated. The activation energy of $NiWO_4$ - WO_3 composites were 0.69, 0.42, 0.56, 0.88, 0.48 eV respectively. In the studied temperature range, the activation energies were found to be low, which predicts that small polaron conduction dominates in this temperature region.

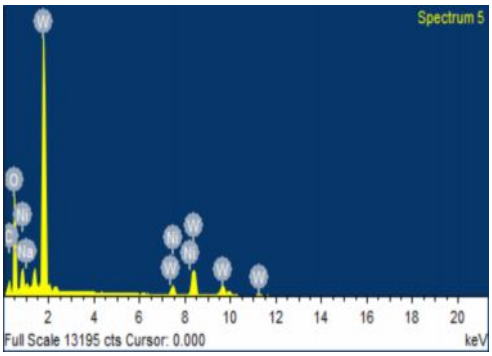

Fig. 1a EDAX spectrum for synthesized $NiWO_4$ – WO_3

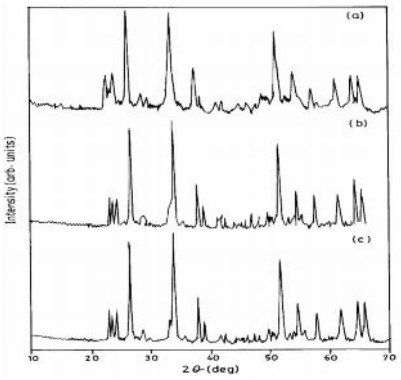

Fig. 1b Powder XRD of $NiWO_4$ – WO_3 composites (a) NWWO-64, (b) NWWO-46 and (c) NWWO-28

As the samples have high resistance (10^8 – 10^4 ohms) and are wide band gap semiconductors, DC current is considered as negligible in the applied voltage of 2–32 V. The lower activation energy predicts that small polaron conduction dominates[30–31] in the temperature range of 373–573 K. In $NiWO_4$ and WO_3 the mobility of charge carriers increases with temperature and hence the conduction is mainly due to small polaron hopping mechanism. In hopping type conduction small polaron move from one impurity site to another by a thermally activated hopping process. The activation energy of $NiWO_4$ single crystals grown by Czochralski method is 0.32 eV. The lower activation energy exhibited in single crystals is due to the more orderliness of the crystal lattices. The lowering of activation energy in transition metal oxides is associated with defects, impurities and interstitials that are generally present in these materials. The defect chemistry of $NiWO_4$ is well understood from the studies also from its distorted scheelite structure.

The resistances of WO_3 and $NiWO_4$ are in the order of 10^8 ohms under dry conditions (RH ~ 5%). It could be inferred from the plot of log *R* vs RH (%) that neither of the terminal phases possesses appreciable sensitivity (Fig. 2) towards moisture when compared to that of the composites. As the humidity is increased, the log *R* values drops and the sensitivity of the elements towards humidity increases. The sensitivity factor (S_f) was calculated from the ratio $R_{5\%}/R_{98\%}$, where $R_{5\%}$ and $R_{98\%}$ are the DC resistances at 5 and 98 % RH respectively (Table. 1).

The sensitivity factor of the $NiWO_4$ and WO_3 composite 459 (NWWO-82), 827 (NWWO-64), 15535 (NWWO-46) and 785 NWWO-28 composite is respectively, with NWWO-46 having the highest S_f value. The significant features of these composites are that the variation in log *R* with RH (%) is almost linear in the entire range of study, a prerequisite for commercial humidity sensors. The sensitivity factor of the composition should be indicative of the extent of moisture condensation in the pores. The SEM photographs (Fig. 3) of the composites NWWO-46 with the same magnification suggested the biphasic nature of the composites and the development of the pore structures with increasing WO_3 content.

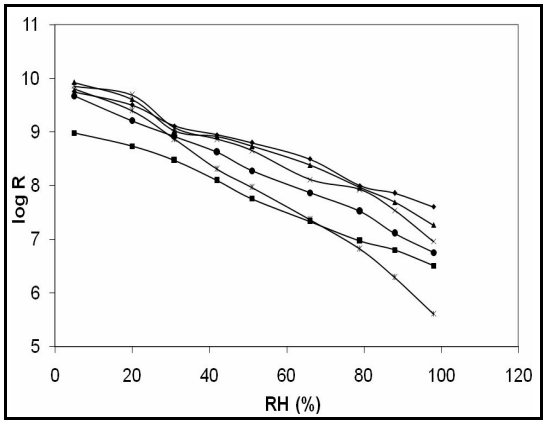

Fig. 2 RH vs log R plot of $NiWO_4$–WO_3 composites

This is further evidenced from the rapid transient in the recovery and response characteristics indicative of physisorption of water molecules on the oxide surface (Fig. 4). When the materials are placed in the higher humid environment, the micropores in the samples will be saturated with water molecules. Due to this the conductivity increases and the resistance decreases causing the variation of S_f with different compositions of the composite.

Summary and Conclusion

The composites of $NiWO_4$–WO_3 in different mole % ratios were prepared by high temperature solid state method. The prepared composites and characterized by powder X-ray diffraction, scanning electron microscope, electrical conductance and humidity sensor studies. The composites were tested as candidate materials for humidity sensing by measuring the variation in their DC resistance as a function of relative humidity in the range of 5-98 % at 25^oC under static conditions. The sensitivity factor, S_f ($R_{5\%}/R_{98\%}$) for $NiWO_4$ and WO_3 composites

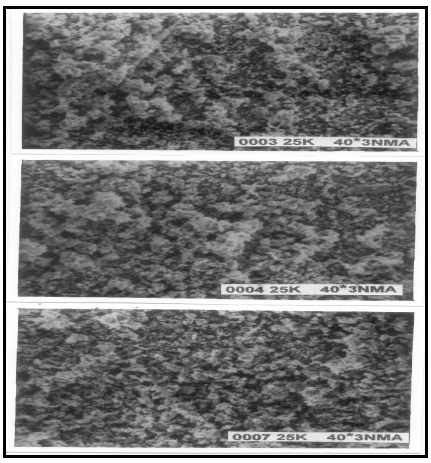

Fig. 3 SEM photographs of $NiWO_4$ – WO_3 Composites. (a) NWWO-64, (b) NWWO-46 and (c) NWWO-28.

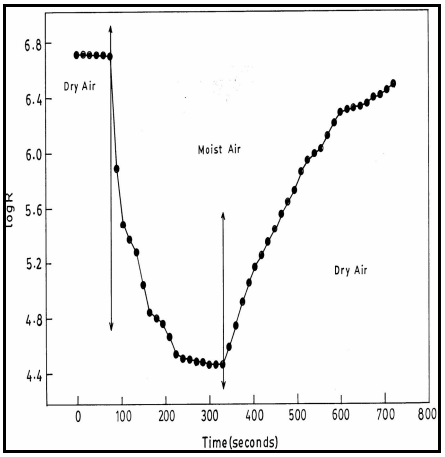

Fig. 4 Response and recovery behaviour of NWWO- 46 composite.

Table 1 Sensitivity factor and Activation energy for $NiWO_4$ – WO_3 composite

No. of moles		Sample code	Resistance $R_{5\%}$ (Ω)	Resistance $R_{98\%}$ (Ω)	S_f ($R_{5\%}/R_{98\%}$)	Activation energy Ea (eV)
$NiWO_4$	WO_3					
100	0	NWWO-10	5.6×10^9	4.05×10^7	138	0.69
80	20	NWWO-82	8.5×10^9	1.85×10^7	459	0.42
60	40	NWWO-64	4.7×10^9	5.65×10^6	827	0.56
40	60	NWWO-46	6.4×10^9	4.11×10^5	15535	0.88
20	80	NWWO-28	7.2×10^9	9.17×10^6	785	0.48
0	100	NWWO-01	9.6×10^9	3.24×10^6	296	0.69

were calculated to be NWWO-82, NWWO-64, NWWO-46 and NWWO-28 is 459, 827, 15535 and 785 respectively. The sensitivity factor of the metal oxide composites NWWO-46 showed a maximum sensitivity (ratio of DC resistance at 5 % RH to that at 98 % RH) of 15535. SEM photograph of the sensor materials sintered at 973 K for 5 h indicated that the porosity and grain size of the materials significantly increases. The scanning electron microscopy (SEM) revealed qualitatively that NWWO-46 composition has greater and larger number of pores in situ level compared to the other composites. In the presence of such gases, cross-sensitivity measurements should be made which, however, is beyond the scope of the present investigation. In the present work, the $NiWO_4$ and WO_3 composites have been proved as effective humidity sensor materials.

Acknowledgement

We thank the Tamil Nadu State Council for Science and Technology (TNSCST), Chennai for financial support (Ref: TNSCST/S & T Projects/AR/PS/2013-2014/2659). The authors are thankful to Dr. Subrata Kundu, ECMS – Division, CSIR - CECRI, Karaikudi for his technical and sample characterization help.

References

1. Saranya S, Senthilkumar ST, Vijaya Sankar K, Kalai Selvan R. Synthesis of $MnWO_4$ nanorods and its electrical and electrochemical properties. J. Electroceram. 2012, 28: 220–225.
2. M.A.P. Almeida, L.S. Cavalcante, M. Siu Li, J.A. Varela, E. Longo. Structural refinement and photoluminescence properties of $MnWO_4$ Nanorods obtained by microwave-hydrothermal synthesis. J. Inorg. Organomet. Polym., 2012, 22: 264–271.
3. Wu W, Qin W, He Y, Wu Y, Wu T. The effect of pH value on the synthesis and photocatalytic performance of $MnWO_4$ nanostructure by hydrothermal method. J. Exp. Nanosci. 2012, 7, 390–398.
4. Zhang E, Xing Z, Wang J, Ju Z, Qian Y. Enhanced energy storage and rate performance induced by dense nanocavities inside $MnWO_4$ nanobars. RSC Adv. 2012, 2: 6748–6751.

5. Chen SJ, Chen XT, Xue Z, Zhou JH, Li J, Hong JM, You XZ. Morphology control of MnWO4 nanocrystals by a solvothermal route. J. Mater. Chem. 2003, 13: 1132–1135.
6. M. N. Mancheva, R. S. Lordanova, D. G. Klissurski, G. T. Tyuliev, B. N. Kunew, J. Phys. Chem. C, 2007, 111: 1101 – 1107.
7. J. M. Quintana – Melgoza, J. Cruz – Reyes, M. Avalos – Borja, Mater. Lett. 2001, 47, 314 – 321.
8. G. A. Niklasson and C. G. Granquist, Electrochromic bragg mirror., J. Mater. Chem., 2007, 17, 127.
9. P. K. Shen, J. Syed - Bokhari and A. C .C. Tseung; J. Elctrochem. Soc., 1991, 138, 2778.
10. S. V. Green, E. Pehlivan, C. G. Granquist and G. A. Niklasson, Sol. Energy Mater. Sol. Cells. 2012, 99, 339.
11. S. H. Lee and S. K. Joo, Sol. Energy Mater. Sol. Cells. 1995, 39, 155.
12. S. H. Lee and Y. S. Park and S. K. Joo, Solid State Ionics, 1998, 109, 303.
13. P. M. S. Monk, S. P. Akhtar, J. Boutevin and J. R. Duffield, Electrochim. Acta. 2001, 46, 2091.
14. N. Penin, A. Rougier, L. Laffont, P. Poizot and J. M. Tarascon, Sol. Energy Mater. Sol. Cells. 2006, 90, 442.
15. D.T. Gillaspie, A. Norman, C. E. Tracy, J. R. Pitts, S. H. Lee, A. Dillon, J. Electrochem. Soc,. 2010, 157, H328.
16. D. T. Gillaspie, R. C. Tenant, and A. C. Dillon, J. Mater. Chem., 2010, 20, 9585.
17. Q. Kuang, C. Lao, Z. L. Wang, Z. Xie, L. Zheng, J. Am. Chem. Soc. 2007, 129, 6070 - 6071.
18. D. Patil, Y. K. Seo, Y. K. Hwang, P. Patil, Sen. Actuators B, 2010, 148, 41 - 48.
19. P. Patil, J. M. Lee, Y. K. Seo, Y. K. Hwang, Y. U. Kwon, S. H. Jhung, J. S. Chang, J. Nanosci. Nanotechol., 2009, 9, 318 - 326.
20. Z. Chen, C. Lu, Sens. Lett. 2005, 3, 274 - 295.
21. Q. Qi, T. Zhang, Q. Yu, R. Wang, Y. Zeng, L. Liu, H. Yang, Sens. Actuators B, 2008, 133, 638-643.
22. X .Q. Fu, C. Wang, H. C. Yu, Y. G. Wang, T. H. Wang, Nanotechnology. 2007, 18, 145503.
23. J. Wang, Q. Lin, R. Zhou, B. Xu, Sens. Actuators B, 2002, 81, 248 - 253.
24. P. M. Faia, C. S. Furtado, A. J. Ferreira, Sens. Actuators B, 2004, 101, 183 - 190.
25. S. Agarwal, G. L .Sharma, Sens. Actuators B, 2002, 85, 205 - 211.
26. G. G. Roberts and F. W. Schmidlin, Phys. Rev., 1969, 180, 785.
27. S. Pokhrel and K. S. Nagaraja, Phys. Stat. Sol. A, 2002, 194, 230.
28. T. Taka, Synth. Met., 1993, 57, 5014.
29. D. Lakshmi and R. Sundaram, Sensors & Transducers, 2008, 97/10, 74.
30. M. Mohanraja and R Sundaram, Journal of Ecotoxicology & Environmental Monitoring, 2008, 18/5, 505.
31. R. Sundaram, Sensors and Actuators B, 2007, 124, 429.

*****